PLD-Grown Y_2O_3 Thin Films from Y Metal: An Advantageous Alternative to Films Deposited from Yttria

M. B. Korzenski,* Ph. Lecoeur,† B. Mercey, D. Chippaux and B. Raveau

Laboratoire CRISMAT, UMR 6508 associé au CNRS, ISMRA et Université de Caen, 6, Boulevard du Maréchal Juin, 14050 Caen Cedex, France

R. Desfeux

Laboratoire de Physico-Chimie des Interfaces et Applications, Université d'Artois, rue Jean Souvraz, SP18, 62307 Lens Cedex, France

Received May 26, 2000. Revised Manuscript Received August 3, 2000

The pulsed laser deposition (PLD) of Y_2O_3 from a pure yttrium ablation target is performed for the first time and is shown to replace advantageously PLD from yttria targets. The films were grown on optical-quality MgO(100) and sapphire(0001) substrates, the former yielding films with poorer crystalline quality because of the large lattice misfit between film and substrate. Regardless of the growth conditions employed, films deposited from the yttrium target consistently exhibit lower ω-rocking curve values than films deposited from the oxide target, thus suggesting a lower degree of tilting between the growth planes of the film. Because of the higher absorption coefficient of the metal target, the metal-deposited films exhibit a smoother film surface than films deposited from the oxide target, which present localized surface outgrowths. The AFM study confirms that the roughness of the films is smaller for Y- than for Y_2O_3-deposited films, but in both cases, it is strongly dependent on the total background gas pressure and on the chemical etching of the substrate surface prior to deposition. Cross-section specimens studied by transmission electron microscopy (TEM) showed that the region near the substrate−film interface is very smooth and that the in-plane orientation of the films changes as a function of film thickness. XPS analysis showed no obvious difference in bonding at the surface of the films deposited from the different targets, indicating that the same level of oxidation occurred during the growth process of the film by each target.

I. Introduction

In recent years, considerable research has been conducted on the growth of yttrium oxide films because of their interesting physical, electronic, and optical properties. The diverse range of potential applications that can be envisioned for Y_2O_3 is quite impressive, including uses as storage capacitors and insulating layers in random access memory (RAM) and metal−insulator−semiconductor (MIS) devices, respectively, because of its large dielectric constant ($\epsilon \approx 17$).[1] Y_2O_3 films also show promise as protective and antireflective coatings for IR detectors because of their robustness (mp = 2410 °C) and efficient transmission of infrared radiation and, most recently, as hosts for rare-earth ions in phosphor displays and waveguide devices. Thus, in light of the vast potential possibilities of Y_2O_3 thin films, significant advances have been made recently in developing a better understanding of the growth and factors that affect the quality and characteristics of Y_2O_3 films in order to optimize their applied potential.

Yttrium oxide exhibits a cubic bixbyte Mn_2O_3 structure and can be described as a calcium fluorite structure with ordered oxygen vacancies; its cell parameter a = 10.60 Å, which closely matches that of Si, for which a = 10.86 Å. Thus, the low lattice misfit (∼2.4%) between Y_2O_3 and Si makes it an attractive candidate as an epilayer for Si in microelectronic devices.[2] For this reason, extensive studies on the growth, crystallinity, and morphology of Y_2O_3 films on Si substrate have been conducted in recent years.[2−5] However, although silicon allows for a low lattice misfit with Y_2O_3 films, it exhibits a relatively high absorption coefficient (13.8 mm^{-1})[3] and refractive index, which could result in a significant loss of light in Y_2O_3 phosphor and waveguide devices. Therefore, several requirements must be considered when a substrate for the growth of thin films for optical applications is selected, which include the following: good transmission of a wide range of light, a refractive index lower than that of the growing film, low cost, availability in large dimensions, and good thermal and

* Author to whom correspondence should be addressed. E-mail: michael.korzenski@ismra.fr.

† Also at LUSAC, Site Universitaire de Cherbourg, 50130 Octeville Cedex, France.

(1) Sharma, R. N.; Rastogi, A. C. *J. Appl. Phys.* **1992**, *71*, 5041.

(2) Zhang, S.; Xiao, R. *J. Appl. Phys.* **1998**, *83*, 3842.

(3) Cho, K. G.; Kumar, D.; Holloway, P. H.; Singh, R. K. *Appl. Phys. Lett.* **1998**, *73*, 3058.

(4) Jones, S. L.; Kumar, D.; Singh, R. K.; Holloway, P. H. *Appl. Phys. Lett.* **1997**, *71*, 404.

(5) Hunter, M. E.; Reed, M. J.; El-Masry, N. A.; Roberts, J. C.; Bedair, S. M. *Appl. Phys. Lett.* **2000**, *76*, 1935.

10.1021/cm001094e CCC: $19.00
Published on Web 09/29/2000

lattice match with the chosen film. Both MgO and sapphire are attractive substrates for the growth of Y_2O_3 films because they satisfy almost all of these necessary requirements, the exception being lattice misfit; however, this may or may not present a problem depending on the specific application of interest. For example, these substrates are cheap and readily available in large sizes, highly transparent, thermally match well with Y_2O_3, and exhibit a low refractive index. The latter becomes very important in waveguide configurations for which a large refractive index contrast between substrate and film results in high confinement of the optical transmission in the guide, leading to efficient pumping and amplification.

A variety of physical and chemical methods have been used over the past decade to synthesize dielectric Y_2O_3 films. These include methods such as chemical vapor deposition (CVD),[6] rf magnetron sputtering,[7] ion-assisted evaporation,[8] anodization,[9] electron-beam evaporation,[10] sol−gel techniques,[11] and reactive synthesis.[12] However, in recent years, pulsed laser deposition (PLD) has proven to be a very attractive and practical method for the growth of high-quality doped[13] and undoped[2] Y_2O_3 films. In this method, either pure or doped Y_2O_3 sintered targets were used for deposition. In the present study, we investigate the possibility of using a pure yttrium metal target for pulsed laser deposition. Our motivation for using a pure metal ablation target, as opposed to yttria, is derived from several possible advantages it may have over the latter. In laser ablation, the target material is ablated, forming atomic species that are subsequently oxidized in the plume expansion by the reactive O_2 gas in the deposition chamber.[14] Therefore, the high absorption coefficient, density, and affinity of yttrium to oxygen should allow for the laser ablation and subsequent growth of thin films of quality and growth rate superior to those grown from a bulk oxide target. Both of these advantages will become important in scale-up processing of micron-thick films for device applications. Furthermore, exploiting the advantages of alternate-target PLD coupled with the use of a metal target can allow for precise control of dopant concentration levels and in-depth separation to optimize performance efficiency in optical planar waveguides.[15] Such control of dopant incorporation would be quite difficult to obtain in single pre-doped oxide targets. Moreover, the use of alternate PLD with metal targets to prepare electroluminescence (EL) and waveguide devices will eliminate the need for lengthy, and sometimes inaccurate, ceramic target preparations. Therefore, the objective of this investigation is twofold: first, to compare the growth of Y_2O_3 films on optical-quality single-crystal MgO(100) and Al_2O_3(0001) substrates and, second, to present a comparison of growth rate, surface quality, and film structure between films deposited from yttrium metal and Y_2O_3 ablation targets (which will be herein referred to as the Y target and the YO target, respectively) by the PLD technique. Such a study has not been pursued before and thus merits investigation in order to expand the synthetic realm of the PLD technique.

II. Experimental Section

Target Preparation. The two different laser ablation targets, yttrium metal and Y_2O_3, used in the following study were 2 cm in diameter and 5 mm thick. The Y_2O_3 target was prepared by mixing Y_2O_3 powder (99.99%) and Ag_2O (10 wt %) in ethanol and ball-milling for 2 h. The Ag_2O served as a flux in order to synthesize a higher-density target.[16] The dried powder was then uniaxially cold-pressed into a disc-shaped pellet and subsequently calcined at 1000 °C in air for 12 h to remove the flux. The target was then sintered at 1450 °C for 48 h in air and then slowly cooled to room temperature at a rate of 1 °C/min to avoid cracking. The target surface was then mechanically polished prior to being used in the PLD chamber. The yttrium metal (99.99%; Kurt J. Lesker Co.) target, with density 4.47 g cm^{-3}, was used as purchased without further preparations. All targets were cleaned prior to each deposition by ablation under the deposition atmosphere with 300−500 pulses to ensure a homogeneous surface morphology and to remove any surface oxide in the case of the metal target.

Thin Film Deposition. Films were typically deposited using a KrF excimer laser ($\lambda = 248$ nm) with an energy density of approximately 2.75 J/cm^2 at various pulse frequencies ranging from 2 to 8 Hz. The laser beam was incident on the target at an angle of 45° from the normal, and the substrate was set at a distance of 45 mm parallel from the target. All films studied in this report were held at a constant temperature of 700 °C during deposition. The substrates were ultrasonically cleaned prior to deposition in acetone and alcohol and then attached to the heating block using silver paste. The chamber was turbopumped to a base pressure of 8×10^{-6} Torr prior to being back-filled with different partial pressures of O_2 in an O_2/Ar gas mixture. The targets were continuously rotated in order to scan the laser beam on the target surface during the deposition process to reduce the possibility of stoichiometric changes in the material. After deposition was completed, the argon gas was purged from the PLD chamber, the oxygen pressure was increased to a static value of 500 mbar, and the films were cooled to room temperature at a rate of 15 °C/min. The argon gas was used in the following studies for manipulation of the laser-ablated plasma size and length and was determined necessary when such low pressures of oxygen gas were used. As will be discussed later in more detail, it also resulted in better film quality.

Characterization. *Surface profile measurements* were run on samples 5×5 mm in size using a Dektak^{3}ST surface profile measuring system to determine the thickness of the Y_2O_3 films. The films were first cleaned with pure alcohol, and then a line with dimensions of 1×5 mm was subsequently chemically etched in the center of the film down to the substrate surface using H_2SO_4 (12%) acid. The total thickness was calculated by taking the average of several profile scans of different regions of the film.

X-ray diffraction (XRD) in the $2\theta-\omega$ scan mode and rocking curve measurements were acquired using a Seiffert XRD-3000

(6) Sharma, R. N.; Rastogi, A. C. *J. Appl. Phys.* **1993**, *74*, 6691.
(7) Gurvitch, M.; Manchanda, L.; Gibson, J. M. *Appl. Phys. Lett.* **1987**, *51*, 919.
(8) Cho, M.-H.; Ko, D.-H.; Jeong, K.; Lyo, I. W.; Whangbo, S. W.; Kim, H. B.; Choi, S. C.; Song, J. H.; Cho, S. J.; Whang, C. N. *J. Appl. Phys.* **1999**, *86*, 198.
(9) Goldstien, R. M. In *Proceedings of the Electronic Components Conference*; Institute of Electrical and Electronics Engineers: New York, 1968; p 141.
(10) Fukumoto, H.; Imura, T.; Osaka, Y. *Appl. Phys. Lett.* **1989**, *55*, 360.
(11) Rao, R. *Solid State Commun.* **1996**, *99*, 439.
(12) Andreeva, A. F.; Sisonyuk, A. G.; Himich, E. G. *Phys. Status Solidi* **1994**, *145*, 441.
(13) Gao, H.-J.; Kumar, D.; Cho, K. G.; Holloway, P. H.; Singh, R. K.; Fan, X. D.; Yan, Y.; Pennycook, S. J. *Appl. Phys. Lett.* **1999**, *75*, 2223.
(14) Dye, R. C.; Muenchausen, R. E.; Nogar, N. S. *Chem. Phys. Lett.* **1991**, *181*, 531.
(15) Serna, R.; Jimenez de Castro, M.; Chaos, J. A.; Afonso, C. N. *Appl. Phys. Lett.* **1991**, *75*, 4073.
(16) Kumar, D.; Sharon, M.; Pinto, R.; Apte, P. R.; Pai, S. P.; Purandare, S. C.; Gupta, L. C.; Vijayaraghavan, R. *Appl. Phys. Lett.* **1993**, *62*, 3522.

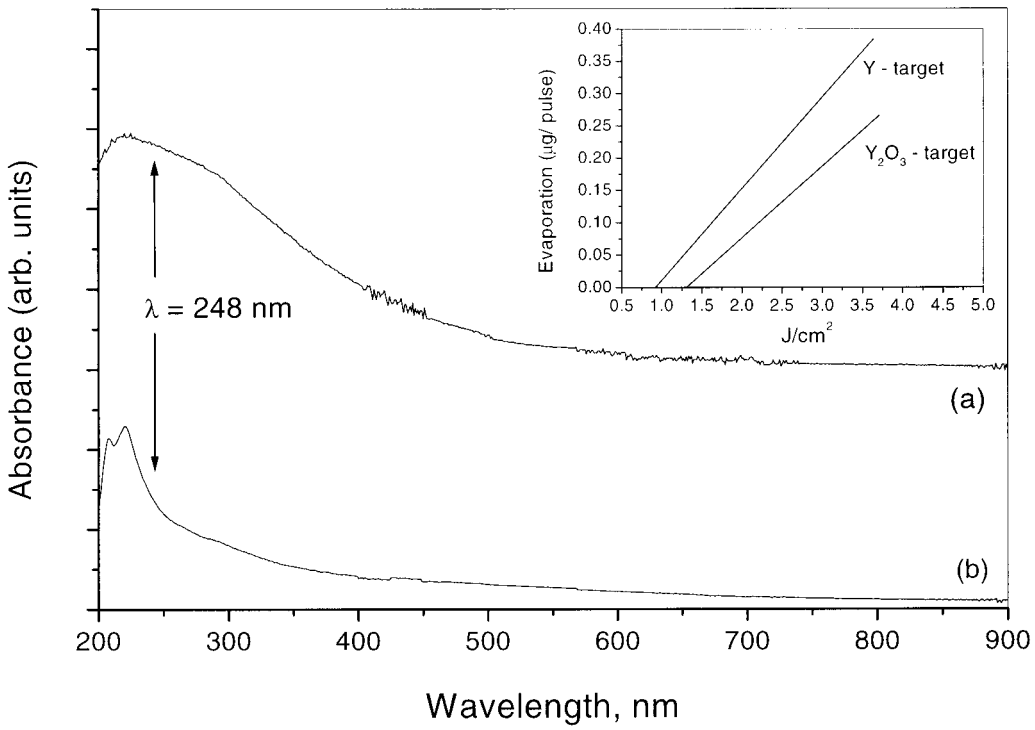

Figure 1. Room-temperature optical absorption spectra of the (a) Y and (b) Y_2O_3 laser-ablation targets. The inset displays the target mass loss by thermal evaporation of the pulsed laser as a function of laser density (J/cm^2). The experiments were run at room temperature with a laser repetition rate of 8 Hz and a gas mixture of 6 mTorr of O_2 and 244 mTorr of Ar.

diffractometer with Cu $K\alpha_1$ radiation. Measurements of the in-plane alignment and crystallinity of the films were carried out using a Philips X'Pert MRD diffractometer.

Atomic force microscopy (AFM) was carried out in air at room temperature by using a Park Autoprobe CP scanning force microscope operating with an optical deflection sensor force. AFM imaging was performed in contact mode with microfabricated Si_3N_4 cantilevers and Si ultralever tips employing a small repulsive force.

Transmission electron microscopy (TEM) was carried out using a JEOL 2010 FX microscope operating at 200 kV. Cross-section specimens were obtained by mechanical grinding and polishing **of** the samples**,** followed by Ar-ion beam milling under a grazing incidence angle of ~10° and an initial beam voltage of 5 kV, which was gradually reduced for the final milling stage.

Scanning electron microscopy (SEM) was performed on a Phillips XL 30 series scanning electron microscope (SEM). The micrographs were acquired from as-grown Y_2O_3 films using a gun voltage of 5 kV to avoid charge build-up due to the insulating nature of the films.

X-ray photoelectron spectroscopy (XPS) investigations were conducted on a Leybold hemispherical analyzer checked on copper, silver, and gold samples, which fit better than 0.1 eV with literature values for a relative resolution of about 1%. Spectra were obtained at a constant pass energy of 50 eV with a nonmonochromatized Mg source in an analysis chamber with a base pressure of 6×10^{-10} Torr. Samples were cleaned in ethanol but not sputtered with Ar^+ ions in order to prevent reduction problems.[17] The physisorbed oxygen peak was used as the internal energy reference, and its position at $E_B = 531.2$ eV was determined on an MBE-grown Y_2O_3 film in situ without any substrate charge.

Ultraviolet/visible spectroscopy (UV/vis) was performed using a Varian Cary 100 Scan UV/visible spectrophotometer in diffuse reflectance mode to obtain absorption spectra of the ablation targets. The scans were obtained in the range from 200 to 900 nm (6.2−1.38 eV) using barium sulfate as the reflectance standard.

(17) Briggs, D.; Seah, M. P. In *Practical Surface Analysis by Auger and X-ray Photoelectron Spectroscopy*; Wiley and Sons: New York, 1987; p 161.

III. Results and Discussion

Film Thickness as a Function of Ablation Target. Most applications of the PLD method will require films grown with a high degree of thickness and compositional uniformity over the entire dimension of the substrate; therefore, growth rate and control of film composition become important control parameters of the PLD process. Thus, the thickness of the Y_2O_3 films was determined from three films prepared with all deposition parameters maintained at constant values, except for the number of laser pulses used in order to verify the reproducibility of the growth rate. The average thickness was calculated by taking the average of several scans with a profilometer at different regions of the film. On the MgO(100) substrate, the deposition rates obtained were 1.1 and 0.85 Å/pulse for the Y and YO targets, respectively, and 1.38 and 1.17 Å/pulse, respectively, for films grown on sapphire(0001). The higher deposition rate (~23%) from the Y target is expected, because of the larger absorption of radiation in the UV/vis region by yttrium metal as compared to Y_2O_3. In fact, at 248 nm, the laser wavelength used for the deposition of the films, the metal target absorbs almost four times as much of the incident radiation as the oxide target (Figure 1). Thus, the absorption of less laser energy results in a lower density of ablated species in the ablation plasma that can subsequently be transferred to the substrate, hence, yielding a lower deposition rate. This was confirmed by measuring the amount of evaporation of the two different targets, and the results are illustrated in the inset in Figure 1. A series of experiments were run with the background gas pressure in the deposition chamber and pulse rate of

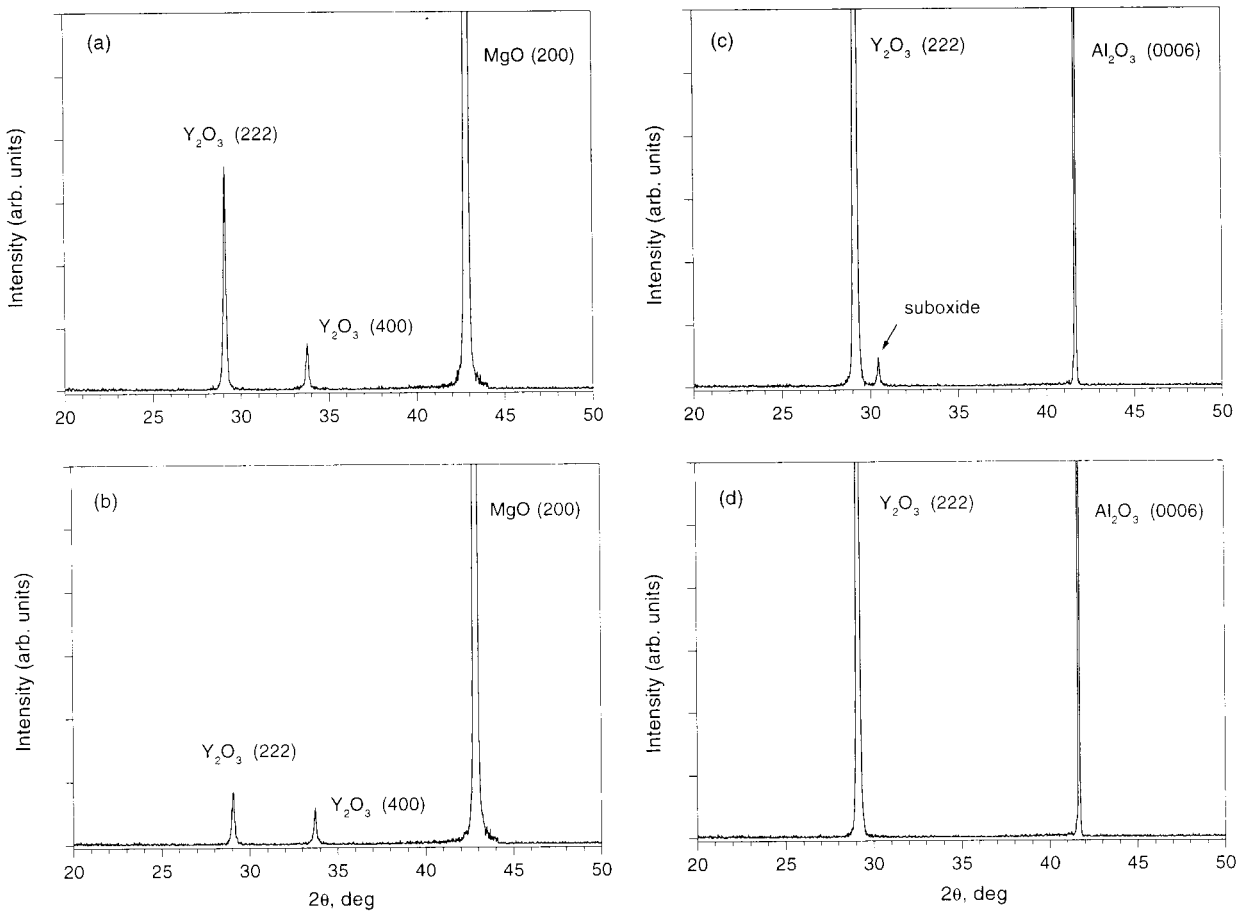

Figure 2. X-ray diffraction patterns of the Y_2O_3 films deposited on MgO(100) from (a) the Y target and (b) the Y_2O_3 target and films deposited on sapphire(0001) from (c) the Y target and (d) the Y_2O_3 target. The deposition conditions were fixed at 700 °C with a gas mixture of 6 mTorr of O_2 and 244 mTorr of Ar.

the laser maintained constant at 250 mTorr and 8 Hz, respectively, while the laser fluence on the two targets was varied. It is clear from Figure 1 that the amount of evaporated target species is higher for the metal target by an average of 27%. This confirms our previous statement that the use of metal targets will permit the transport of more ablated species to the substrate. Moreover, in general, PLD films grown from highly absorbing target materials exhibit a smoother surface quality than films deposited from less absorbing materials.[18] This was observed in the AFM measurements and will be discussed in detail later.

X-ray Diffraction Analysis of Y_2O_3 Structure. The $\theta-2\theta$ X-ray diffraction (XRD) patterns for Y_2O_3 films deposited on MgO(100) and sapphire(0001) at 700 °C using the Y- and YO-ablation targets is shown in Figure 2. All four depositions were performed using the following growth parameters: 4 Hz, 2.75 J cm^{-2}, 250 mTorr of O_2/Ar background gas mixture containing 2.5% O_2, with changes only in the number of laser pulses on each target to produce films with identical thickness. The YO-deposited film on MgO (Figure 2b) shows film growth in both the [111] and [100] directions and is similar to results previously reported by Zhang and Xiao[2] for Y_2O_3 films deposited on fused silica substrates under similar temperature and oxygen pressure conditions. Figure 2a shows the Y_2O_3 film deposited from the Y target, and it is clear from the XRD pattern that the film is more crystalline, as observed by the 4-fold increase in the intensity of the (222) diffraction peak. Moreover, the (222)/(400) peak ratio is 5:1, compared to 1.4:1 for the YO-deposited film. This shift in intensity is attributed to the fact that the (111) orientation of Y_2O_3 contains ordered oxygen vacancies and, thus, is the preferred direction of growth when the Y target is used because of the lower concentration of oxygen in the ablated plasma during deposition compared to that in the YO-ablated plasma. This was confirmed by performing a series of depositions with the percent of oxygen in the background gas varied from 0 to 75% during separate depositions of Y_2O_3 films on MgO using the Y target. At oxygen concentrations below 10%, the (400) diffraction line is no longer observed in the film; however, as the O_2 pressure was increased above this value the film transformed from being dominated by the (222) orientation to being dominated by the (400) orientation, because fewer oxygen vacancies were available in the growing film. Other groups have observed similar changes in orientation both during deposition of the film and in postannealing processes.[2,4,19,20] Meanwhile, the intensity of both diffraction peaks decreased.

The X-ray diffraction pattern of Y_2O_3 grown on sapphire from the Y target (Figure 2c) shows a mixture

(18) Haumesser, P. H.; Théry, J.; Daniel, P. Y.; Laurent, A.; Perrière, J.; Gomez-San Roman, R.; Perez-Casero, R. *J. Mater. Chem.* **1997**, *7*, 1763.

(19) Huignard, A.; Aron, A.; Aschehoug, P.; Viana, B.; Théry, J.; Laurent, A.; Perriere, J. *J. Mater. Chem.* **2000**, *10*, 549.

(20) Jollet, F.; Noguera, C.; Gautier, M.; Thromat, N.; Duraud, J. P. *J. Am. Ceram. Soc.* **1991**, *74*, 358.

consisting of a very intense diffraction line located at $2\theta = 29.18°$ due to the Y_2O_3 (222) plane normal to the substrate surface and a peak of very weak intensity at $2\theta = 30.68°$. The former corresponds to a *d* spacing of 3.058 Å and is in perfect agreement with the standard value for stoichiometric bulk Y_2O_3. However, the latter corresponds to a *d* spacing of 2.91 Å and is not related to any crystallographic orientations within cubic Y_2O_3. Thus, taking into consideration the absence of oxygen in the metal target and the low partial pressure of oxygen gas present during the deposition, this peak is assumed to be an artifact of an oxygen-deficient phase. In fact, a *d* spacing of 2.91 Å is in good agreement with the (101) orientation of the unit cell of the suboxide $YO_{1.34}$, which has hexagonal symmetry[21] (space group $P6_3/mmc$ with $a = 3.810$ Å and $c = 6.034$ Å). Although Craciun and co-workers[22] have observed a similar peak present in ultraviolet-assisted PLD (UVPLD) grown Y_2O_3 films deposited from the Y_2O_3 target, we have never observed this diffraction peak in any of our YO-deposited films. The X-ray diffraction pattern for the YO-deposited film (Figure 1d) reveals only the (222)-oriented diffraction line and no other diffraction peaks, indicating that the film is uniaxially textured along this direction. However, the normalized intensity is 4 orders of magnitude weaker than the same diffraction peak for the Y-deposited film, suggesting lower out-of-plane crystallinity.

It should be noted that the Y-deposited films reproducibly exhibit an out-of-plane *d* spacing that is, depending on the substrate used, either closer to or identical to the bulk value of 3.058 Å for the (222) peak in Y_2O_3, as compared to the YO-deposited films. For instance, the observed out-of-plane parameter, *d*, for the (222) diffraction peak of Y-deposited films grown on sapphire is consistently 3.058 Å ($2\theta = 29.18°$), matching exactly that of the bulk Y_2O_3 target. Meanwhile, the YO-deposited films on the same substrate yield a slightly larger value of 3.062 Å ($2\theta = 29.14°$). On MgO substrates, the *d* spacings are 3.064 Å ($2\theta = 29.12°$) and 3.070 Å ($2\theta = 29.06°$) for the Y- and YO-deposited films, respectively. The fact that films grown on MgO result in larger (222)-peak *d* spacings than films grown on sapphire is consistent with the decrease in lattice misfit. Although the misfit is large for both substrates, the extremely large misfit on MgO causes severe in-plane compression in the epilayers and subsequently results in a larger out-of-plane *d* spacing. In most cases, a large lattice misfit is deleterious to the crystallinity of the growing film, but we observe that the compressive stress shown by the film might aid in relaxing the film in the direction perpendicular to the substrate and, thus, possibly in reducing the propensity for crack formation. This suggestion is currently under more detailed investigations via transmission electron microscopy.

Changes in Film Crystallinity and Surface Quality as a Function of Growth Pressure and Postannealing Processes. To improve the quality of the Y_2O_3 films, a study of total background pressure was undertaken to determine its effect on the crystallinity and surface morphology of the deposited films. We have previously mentioned that increasing the oxygen pressure in the background gas during deposition not only alters film orientation, but also gradually decreases film crystallinity as well. However, by maintaining the O_2 pressure at the optimal pressure for crystallization, 6 mTorr, while changing the Ar pressure, we have successfully optimized film crystallinity. As the total background pressure increases, the laser-ablated plasma becomes longer and narrower, and thus, the plasma front becomes highly localized on the surface of the growing film. As shown in Table 1, the intensity of the (222)-oriented diffraction peak significantly increases as the amount of argon in the background gas mixture is raised from 0 to 400 mTorr. This can be explained by a longer *residence time* of the ablated species in the plasma.[23] For example, the longer residence time allows more time for the plasma species to form large particulates and more time for these particulates to migrate on the growing film surface before being covered by the next incoming plasma; in turn, this will lead to better film quality. Evidence in favor of this argument comes from the fact that the suspected suboxide peak at $2\theta = 30.68°$ gradually disappears as the total background pressure during deposition is raised, indicating that the particulates, either in-flight or on the growing film surface, have a longer time to be efficiently oxidized. It is important to note here that the same growth pressure using pure O_2 produces rough films with an amorphous characteristic. Therefore, by employing an argon-rich growth atmosphere, a high degree of film crystallinity and stoichiometry can be achieved.

Table 1. Effects of Total Background Pressure on the (222)-Oriented Diffraction Peak of a Y-Deposited Film Grown on Sapphire(0001) at 700 °C

P_{O_2}/P_{Ar} (mTorr)	*d* spacing (Å)	$I_{(222)}$ (cps)	ω-scan fwhm (°)
6/0	3.100	80	–
6/200	3.062	2200	1.42
6/300	3.058	5700	1.34
6/400	3.058	14500	1.05
6/500	3.062	1900	2.09

Table 2. Rocking Curve fwhm of Films Grown at 700 °C as a Function of Target, Substrate, and Laser Frequency Employed

target	substrate	laser frequency (Hz)	T_{anneal} (°C)	ω-scan fwhm (°)
Y	MgO(100)	2	–	1.85
	MgO	4	–	2.21
	MgO	8	–	2.71
	sapphire(0001)	2	–	1.05
	sapphire	2	800	1.03
	sapphire	2	1000	0.90
	sapphire	2	1200	0.87
Y_2O_3	MgO(100)	2	–	2.14
	MgO	4	–	3.06
	MgO	8	–	3.44
	sapphire(0001)	2	–	1.38
	sapphire	2	800	1.26
	sapphire	2	1000	1.17
	sapphire	2	1200	0.86

Postannealing in an oxygen ambient at 800, 1000, and 1200 °C for 1 h significantly increases the crystallinity of the films, as confirmed by the fwhm values of the rocking curve measurements listed in Table 2. The XRD pattern of the films annealed at 800 °C clearly showed an enhancement in crystallinity, and surface analysis of the films using a polarized optical microscope showed no signs of visible crack formation in the films after the thermal annealing process. However, when the films

(21) Solov'eva, A. *Inorg. Mater.* **1985**, *21*, 701.
(22) Craciun, V.; Lambers, E. S.; Bassim, N. D.; Singh, R. K. *J. Mater. Res.* **2000**, *15*, 488.

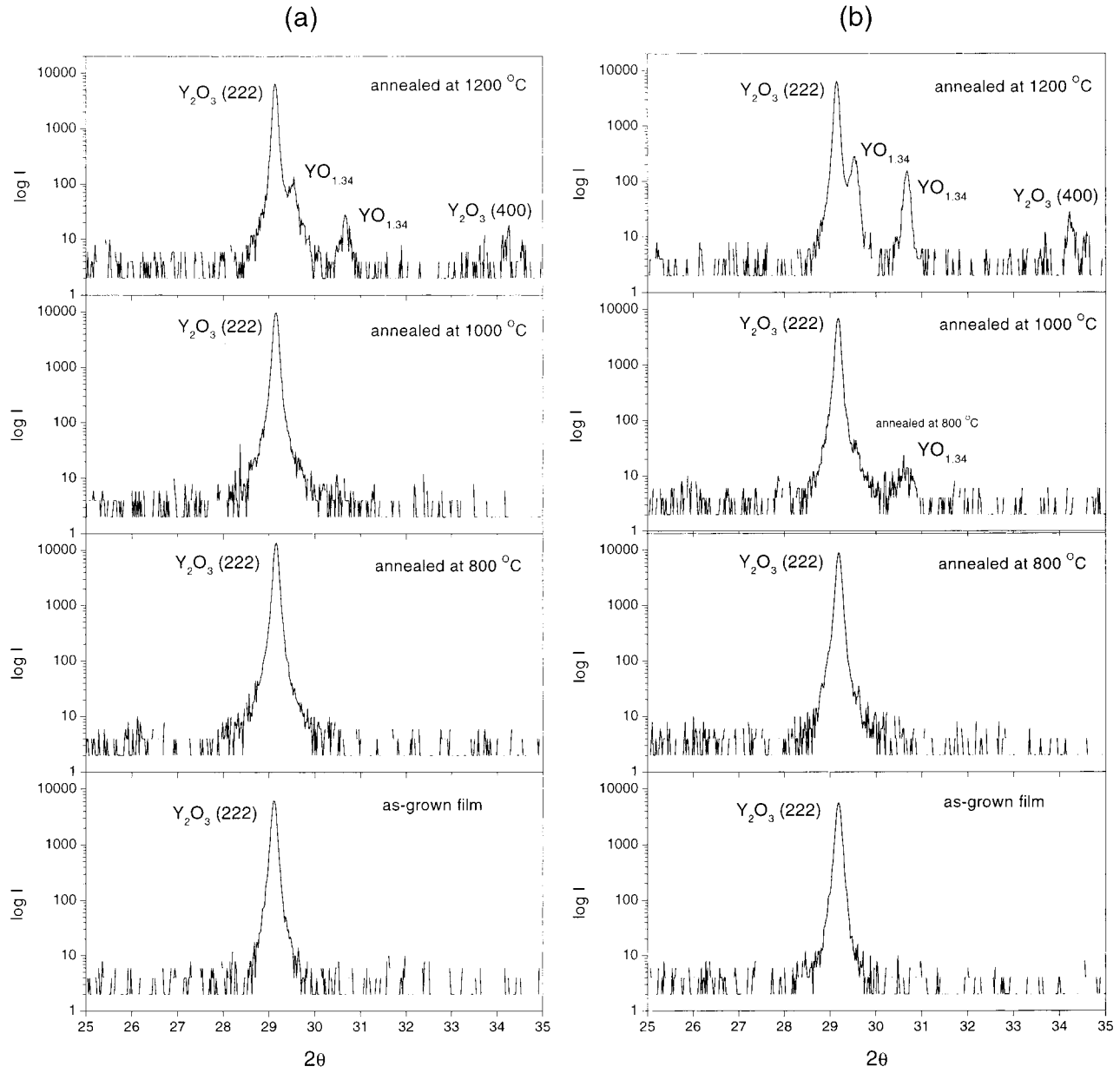

Figure 3. XRD diffraction patterns of the (a) YO-deposited and (b) Y-deposited Y_2O_3 films (deposited on sapphire) postannealed in oxygen ambient at 800, 1000, and 1200 °C for 1 h. The deposition conditions used for the growth of the films were 700 °C, 6 mTorr O_2, 244 mTorr Ar, 4 Hz, and 2.75 J cm^{-2}.

were subjected to annealing at temperatures above 1000 °C, several new diffraction peaks appear (Figure 3) as a result of the increased density of the films. Nonetheless, the advantage of both MgO and sapphire substrates compared to Si in postannealing processes and high-temperature depositions (>675 °C) is that, unlike Si, they do not undergo solid-state reactions with the film when subjected to elevated temperatures (>700 °C). For example, Sharma and co-workers[2] have previously reported that, when electron-beam-evaporated Y_2O_3 films were subjected to annealing temperatures above 675 °C, solid-state reactions were initiated between the film and Si substrate, subsequently inducing growth of thermodynamically stable yttrium silicates at the substrate−film interface, particularly $Y_2Si_2O_7$ and $YSiO_2$. Such reactions did not occur with MgO and sapphire, as confirmed by the absence of any interfacial oxide layers in cross-section specimens studied by TEM. This is most likely due to the higher melting point and thermal stability of both MgO and sapphire as compared to Si.

Rocking Curve (fwhm) X-ray Diffraction Analysis of Y_2O_3 Films. The crystallinity of the films was investigated by rocking-curve (ω-scan) measurements. The full width at half-maximum (fwhm) values of the (222) peak of the films, along with various deposition parameters, are listed in Table 2. The measurements yielded large fwhm values of 1.84° and 2.11° for the Y and YO targets, respectively, implying severe tilting of the (111) planes most likely because of stacking faults arising from the large lattice misfit. Nonetheless, the Y-deposited films are seemingly more crystalline than the YO-deposited films, while films deposited on sapphire show much better crystallinity than films deposited on MgO because of the lower lattice misfit of the film and substrate. Also, single-crystal MgO is very hygroscopic, and even when high purity solvents are used during the cleaning processes, there remains some

possibility for hydration of the oxide surface. This will have a drastic effect not only on the film growth, but on the optical properties as well, leading to considerable absorption of light by O−H bands in the infrared region.

The fwhm of the (222) diffraction peak is strongly dependent on the frequency of the pulsed laser and decreases linearly as the rate is decreased from 8 to 2 Hz. This can be explained by the fact that, when the time between laser pulses is increased, the adatoms on the surface of the growing film have enough time to migrate and settle into the orientation of lowest free surface energy before being bombarded by plasma species from the following laser pulse. This would lead to a more dense and well-aligned packing of the preferred (111)-oriented planes in the film, as confirmed by the rocking curve measurements listed in Table 2. Moreover, a lower laser frequency normally results in a diminished density of surface droplets on the surface of the growing film and will thus have a positive effect on the overall crystallinity of the film; however, it will result in a decrease in the film growth rate.[23]

Determination of In-Plane Epitaxial Relationship between Film and Substrate. The in-plane alignment of the Y- and YO-deposited films on sapphire and MgO were obtained performing ϕ scans. The ϕ scan in the range of 0−360° of a Y_2O_3 film grown on MgO-(100) revealed 12 broadened peaks varying in intensity and exhibiting a peak width of 8.08°. The diffractometer resolution measured on the MgO(200) surface was 0.26°. The 12 peaks are separated by a 30° rotation of the unit cells with respect to each other and rotated by a shift of 15° toward the (100) direction of the MgO substrate, indicating multiple in-plane orientations. This is expected because of the existence of both the (222) and the (400) out-of-plane orientations that are always observed regardless of the growth conditions employed. The large fwhm of the peaks is probably a result of substantial twist misalignment of the grains because of the large lattice misfit between Y_2O_3 and MgO.

As the lattice misfit between the substrate and film decreases, as when going from MgO to sapphire, the density of defects present in the growing film and at the film−substrate interface would also be expected to decrease. This was confirmed by a significant reduction of the fwhm (ω scan) values when Y_2O_3 films were grown on sapphire, as mentioned previously. It is clear from Table 1 that the fwhm values of the Y- and YO-deposited films on sapphire(0001) are 43% and 36%, respectively, smaller than the values for films deposited under the same deposition parameters on MgO(100). The effect of the lower lattice misfit is observed in the ϕ scan of Y- and YO-deposited films of equal thickness on sapphire(0001), as shown in Figure 4a and 4b, respectively. In the full ϕ range of 0−360°, both diffraction patterns exhibit six peaks, thus indicating two type-*b* in-plane orientations, similar to the bonding arrangement of CaF_2 on Si(111),[24] with a 60° rotation of the unit cells with respect to one another and 30° rotation of each from the (116) reflection of the substrate, which exhibits a diffractometer resolution of 0.5°. In the Y-deposited Y_2O_3 film, the three peaks in the first set are separated by 120° from one another and have

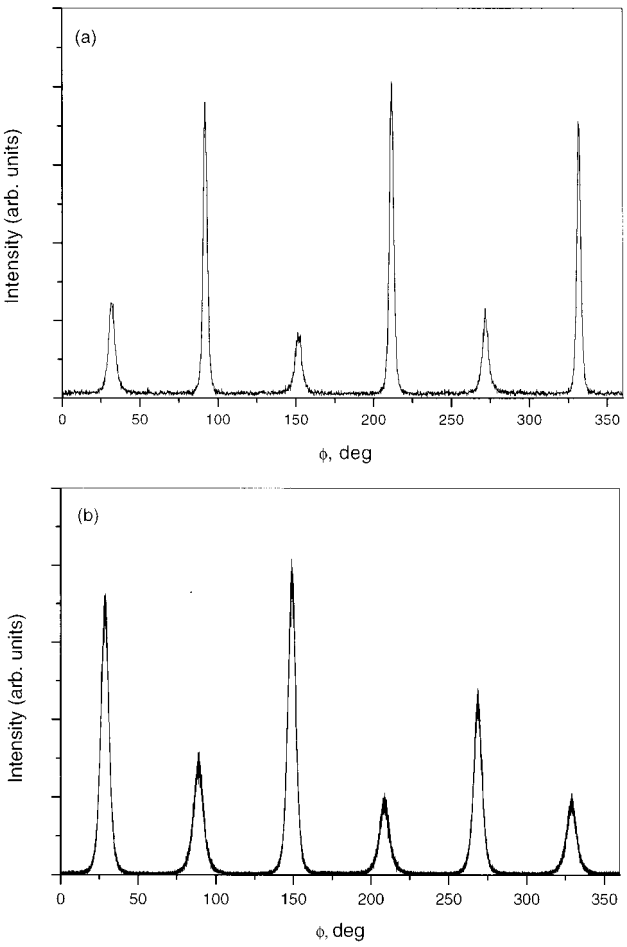

Figure 4. Azimuthal ϕ scan of the (222) reflection for (a) Y-deposited Y_2O_3 film grown on a sapphire(0001) substrate and (b) YO-deposited film under 6 mTorr O_2 and P_T = 250 mTorr. The six substrate peaks from the (116) reflection of sapphire were located at 0°, 60°, 120°, 180°, 240°, and 300° and are not shown for the sake of clarity.

an average fwhm of 4.21°, while the second set of three are more intense and have an average width of 2.77°. On the other hand, the YO-deposited film exhibits the same peak spacing, but the average fwhm values for the intense and weak peaks are 5.45° and 7.81°, respectively. This reinforces the X-ray diffraction data, which previously showed that the YO-deposited films were consistently less crystalline with more tilting of the (222) planes.

To our knowledge, there have been very few reports of an observed cube-on-cube epitaxy of Y_2O_3 films in relation to the substrate, specifically, YSZ(100),[19] LAO-(100),[25] and MgO(110) and (210),[26] which exhibit low lattice misfit values, thus emphasizing the difficulty in growing highly crystalline, cube-on-cube epitaxial Y_2O_3 films. However, the twinning nature of LAO and the large refractive index of YSZ may render these substrates less attractive for some optical applications.

AFM Studies on the Effects of Ablation Target and Growth Pressure. The grain size and surface morphology of the Y_2O_3 films grown on sapphire(0001)

(23) *Pulsed Laser Deposition of Thin Films*; Chrisey D. B., Hubler, G. K., Eds.; Wiley & Sons: New York, 1994; p 456.
(24) Asano, T.; Ishiwara, H. *Appl. Phys. Lett.* **1983**, *42*, 517.
(25) Kumar, D.; Cho, K. G.; Chen, Z.; Craciun, V.; Holloway, P. H.; Singh, R. K. *Phys. Rev. B* **1999**, *60*, 13331.
(26) Edwards, J. A.; Chew, N. G.; Goodyear, S. W.; Satchell, J. S.; Blenkinsop, S. E.; Humphreys, R. G. *J. Less-Common Metals* **1990**, *164−5*, 414.

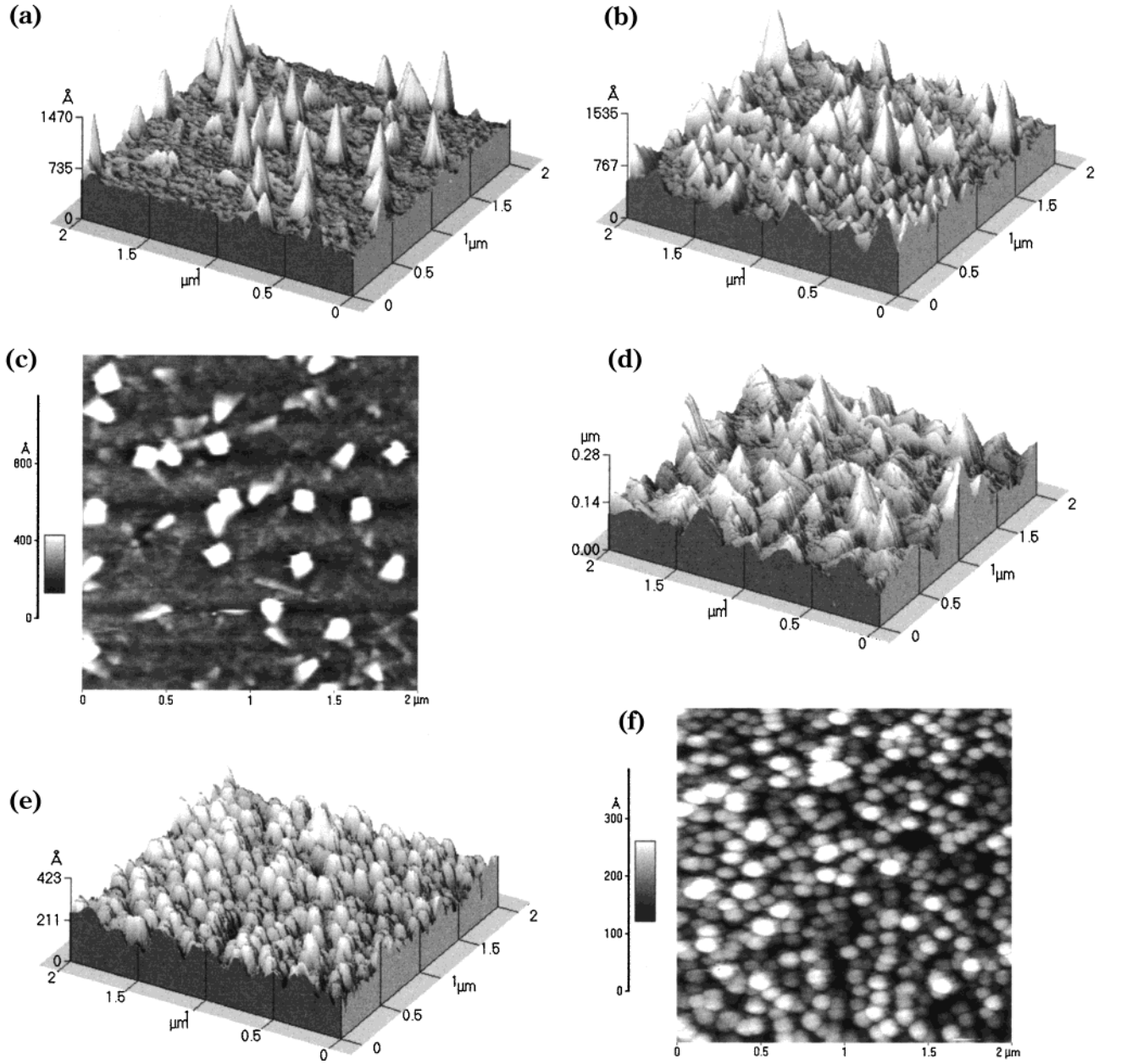

Figure 5. AFM surface images of Y_2O_3 films deposited on a sapphire(0001) substrate at 200 mTorr total growth pressure (6 mTorr O_2) deposited from the (a) Y target and (b) YO target and (c) 2D view of b. AFM surface images of Y_2O_3 films deposited at 500 mTorr (d) on a sapphire(0001) substrate from the Y target and (e) on a chemically etched sapphire(0001) substrate from the Y target and (f) 2D view of e.

deposited from both targets at different growth pressures was measured by AFM. It is clear from the images of both the Y- and the YO-deposited Y_2O_3 films presented in Figure 5a and 5b, respectively, that they exhibit pyramidal-shaped grains that form 3D islands. Figure 5c shows the 2D view of the film presented in Figure 5a and points out the pyramidal shape of the grains. This grain morphology observed is a signature of the crystallographic cubic-fluorite structure of bulk Y_2O_3. The images presented in Figure 5a and 5b display a 3D island growth mode (Stranski−Krastinov) by which an initial monolayer of film is formed, followed by nucleation and subsequent growth of 3D islands.[23] The topological surface measurements (peak−valley height) indicate two in-depth growth regions distinguished from each other by a significant difference in the grain size. The relatively smooth lower region consists of grains with an average size of 70 nm whereupon 3D islands nucleate to form larger grains with an average size of 160 nm. These observations are in good agreement with the X-ray investigations presented previously in which the ϕ scan of the Y_2O_3 films showed two in-plane alignments by the grains of the (111) domains twisted 60° from one another.

The surface roughness of 1-μm-thick Y_2O_3 films taken from a surface area of 2 × 2 μm was ∼9.5 and ∼12.5 nm for the Y- and YO-deposited films, respectively (Table 3). Although these value are relatively high compared to those for Y_2O_3 films grown on a Si substrate[2], the roughness is a film characteristic that can be manipulated by changing the partial pressure of O_2 and the total growth pressure during deposition. Jones et al.[4] have experimentally observed a profound increase in the surface roughness of Eu/Y_2O_3 films when the growth pressure (O_2) was raised from 1×10^{-2} mTorr to values above 400 mTorr; however, confirmation by

Table 3. AFM Analysis of the Grain Size, Surface Roughness, and Peak−Valley Height for the Y_2O_3 Films Grown on Sapphire(0001) as a Function of Target, Background Pressure, and Chemical Treatment of Substrate

target	P_T[a] (mTorr)	grain size (nm)	average roughness (nm)	peak-to-valley height (nm)
Y	200	160/70	9.5	103
Y_2O_3	200	160/70	12.5	112
Y	500	160/70	29.0	222
Y[b]	500	120	4.4	39

[a] The total growth pressure, P_T, results from a fixed O_2 pressure of 6 mTorr and the remaining pressure of Ar gas. [b] Substrate was chemically etched with a 3:1 mixture of a H_2SO_4/H_3PO_4 solution prior to deposition.

X-ray diffraction showed that the films changed from a single growth orientation (111) to a multiply oriented film with a decrease in crystallinity. The authors also found the optimum O_2 growth pressure to be around 200 mTorr for the growth of a high-quality (111)-oriented Eu/Y_2O_3 films. This value is considerably higher than the optimum O_2 pressure of 6 mTorr we have discovered for the growth of Y_2O_3 films exhibiting similar film quality and orientation and can be explained by the difference in the choice of substrate employed. Nonetheless, to maintain a high level of crystallinity and obtain a high surface roughness of the film, at the same time we have investigated the effects of the total background gas pressure by using argon gas as a chemically inert pressure controller. The AFM image shown in Figure 5d shows a substantial increase in the rms value of the Y-deposited film when the total growth pressure during deposition was increased from 200 to 500 mTorr while the O_2 pressure was fixed at 6 mTorr. It is noted that the grain size and shape remained the same even though the X-ray diffraction pattern revealed a large decrease in intensity of the (222) peak (Table 1). Nevertheless, the surface roughness of the film increased by a factor of 2. However, in the X-ray diffraction analysis comparison of the total growth pressure (Table 1), the optimal pressure of crystallization has been shown to fall in the region of 300−400 mTorr. In addition, although no AFM measurements were run on films grown in this region, we would expect to observe a larger grain size for such films in view of the X-ray diffraction intensity observed.

We have also explored the affects of chemically etching the substrate surface on the surface morphology of the film. An etching procedure similar to that reported elsewhere[26] was employed that consisted of heating the sapphire substrate in a H_2SO_4/H_3PO_4 solution and then immediately transferring the substrate to the deposition chamber where it is then annealed in O_2 for 30 min prior to deposition of the Y_2O_3 film. It is important to note here that, although the film was deposited under a high growth pressure (500 mTorr), which we have just shown produces a rougher film surface, the observed rms value was only 4.4 nm. This is almost seven times smoother than the film grown under the same pressure on a nonetched substrate and two times smoother than the film grown under 200 mTorr, while only a small decrease in grain size was observed. Therefore, one might assume that a film prepared on a pre-etched substrate in the growth pressure range 200−400 mTorr (the optimal range for out-of-plane crystallinity) will yield a smooth film

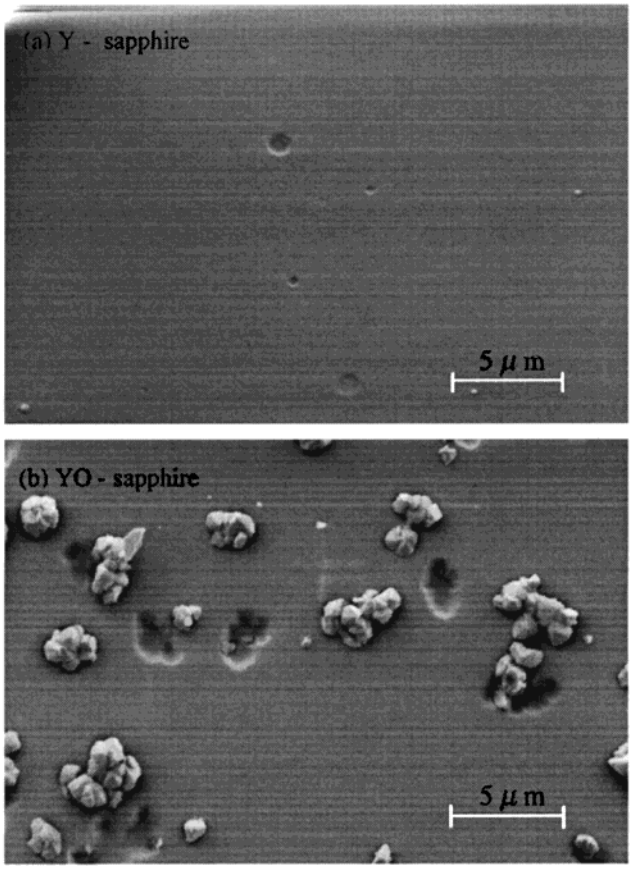

Figure 6. SEM surface view of (a) YO-deposited film and (b) Y-deposited film on a sapphire(0001) substrate.

exhibiting good crystallinity. Moreover, an obvious topographical change in the film surface was also observed, accompanied by a change in grain morphology from pyramidal to spherical. The 3D view of the film shown in Figure 5e and 5f shows a columnar-like growth at the film surface, representative of 2D growth of the film, and is consequently the reason for the smooth surface. Thus, it seems that a reconstruction of the substrate surface prior to deposition has an important effect on the growth mode of the growing film. However, this assumption can only be realized by the use of reflection high-energy electron diffraction (RHEED), which has recently proven to be a powerful tool for the in situ monitoring of films at the initial stages of growth.[27−29]

Scanning Electron Microscopy. Scanning electron microscopy was used as a secondary surface technique in comparison with the AFM measurements to examine the presence and density of macroscopic surface defects such as droplets. The micrographs of the Y_2O_3 films deposited from the yttria and yttrium metal target are presented in Figure 6. As can be seen in Figure 6a, the Y-deposited film is smoother than the YO-deposited film, as was also observed by the AFM measurements discussed previously. Meanwhile, it is interesting to note that the Y-deposited film surface exhibits a much lower density of surface droplets than is typically observed for films deposited from metal targets. The crater-shaped

(27) Chen, Y.; Ko, H.-J.; Hong, S.-K.; Yao, T. *Appl. Phys. Lett.* **2000**, *76*, 559.
(28) Rijnders, G. J. H. M.; Koster, G.; Blank, D. H. A.; Rogalla, H. *Appl. Phys. Lett.* **1997**, *70*, 1888.
(29) Karl, H.; Stritzger, B. *Phys. Rev. Lett.* **1992**, *69*, 2939.

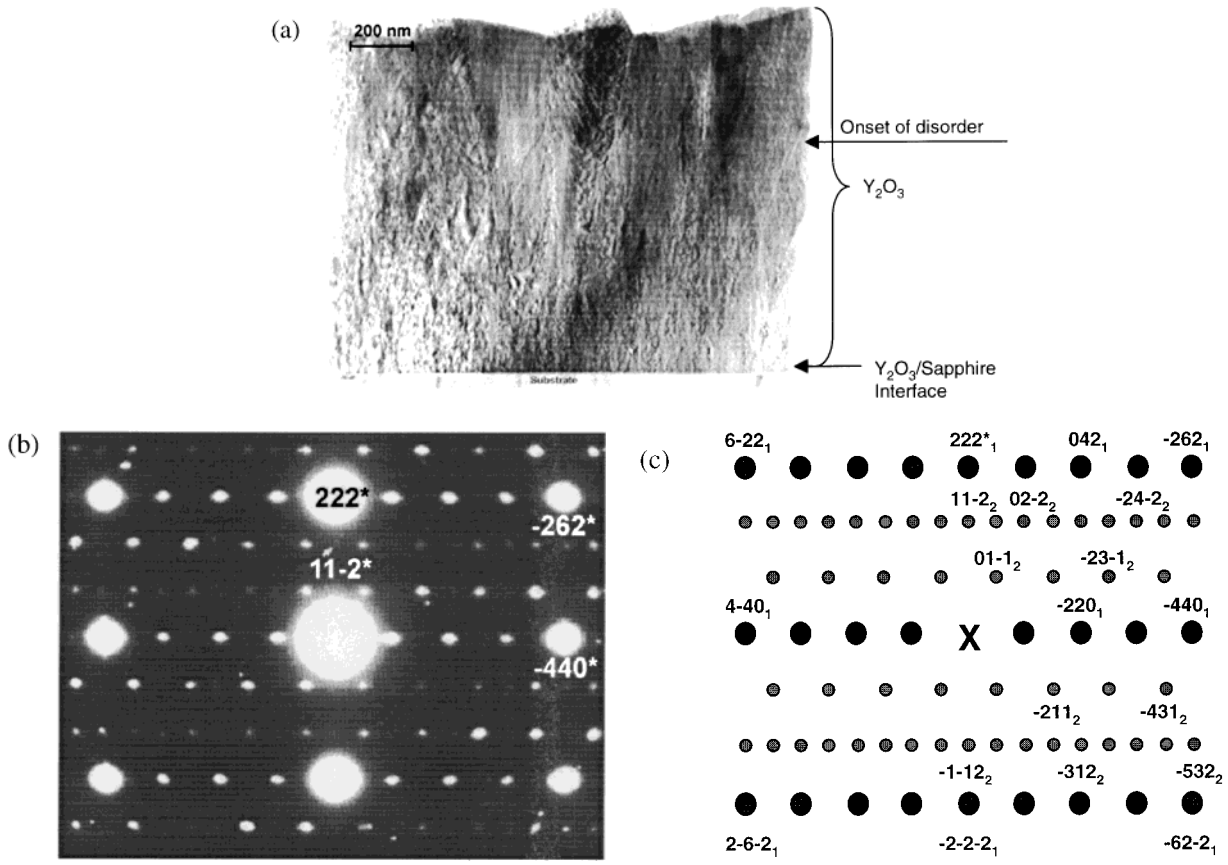

Figure 7. (a) Cross-sectional TEM image of YO-deposited film on sapphire(0001) and (b) ED pattern taken near the interface of the cross section shown in a. To clearly explain the diffraction pattern described in the TEM section of the text, a schematic drawing is presented in c in which the diffraction spots from the two in-plane orientations are labeled by subscript arabic numerals 1 and 2.

holes might be the result of post-deposition evaporation of the laser-induced droplets. Meanwhile, the YO-deposited film contains localized areas on the film surface that exhibit a rather high density of particles (Figure 6b). The particles display well-defined facets, giving rise to an octahedral geometry with an average size of 1 μm. The fact that they are not hemispherical or irregular in shape indicates, respectively, that they are neither surface droplets nor fragments expelled from the target by the explosive impact of the laser, but rather crystallites nucleating from the surface of the film. The formation of localized outgrowths on the film surface could also explain the island growth observed in the AFM measurements and, thus, the poorer crystallinity shown by X-ray diffraction. For instance, macroscopic outgrowths such as those observed in the SEM images would not have sufficient kinetic energy to migrate on the film surface to form a dense homogeneous layer and, therefore, would induce localized defects in the film, consequently resulting in a decrease in film crystallinity.

Transmission Electron Microscopy (TEM). A TEM cross-section image of a YO-deposited Y_2O_3 film grown on sapphire(0001) at 700 °C is presented in Figure 7a. The total thickness of the film as measured by TEM was 1.6 μm and is in good agreement with the predetermined thickness calculated prior to the deposition using the deposition rate of 1.17 Å/pulse, as mentioned previously. It is apparent from the image that the film−substrate interfacial region shows a smooth and sharp interface and that the film orientation and thickness remain constant to a thickness of approximately 1 μm and then clearly change to a highly disordered structure. The surface of the film displays an irregular and rough morphology including valleys that are 200 nm in depth, which is in good agreement with the rough surface of the films observed by AFM. The electron diffraction (ED) pattern of the cross section is presented in Figure 7b. The electron beam is parallel to the [110] direction of the sapphire substrate, and the diffraction was taken from an area in close proximity to the substrate−film interface. Well-defined spots indicating good crystallinity of the film characterize the ED pattern. However, assuming that the Y_2O_3 film has the same structure as the bulk material, the spacing along the direction perpendicular to the substrate plane cannot be interpreted as the result of a single orientation of the film with respect to the substrate. As previously determined by XRD, part of the diffraction pattern can be indexed in the $(1\bar{1}2)$* plane, with the $[\bar{2}22]$* direction perpendicular to the substrate and the $[\bar{1}10]$* direction parallel to the corresponding direction of the substrate (the diffraction spots from this plane are labeled as subscript arabic numeral 1 in Figure 7c). To explain the ED pattern completely, a second plane must be taken into consideration. For instance, the $(11\bar{1})$* plane must be oriented in such a way that the $[11\bar{2}]$* direction is perpendicular to the substrate, thus rendering it parallel to the $[22\bar{2}]$* direction of the former plane. At the same time, the $[\bar{1}10]$* direction is parallel to the corresponding direction of the substrate (diffraction spots from this plane are labeled as subscript arabic

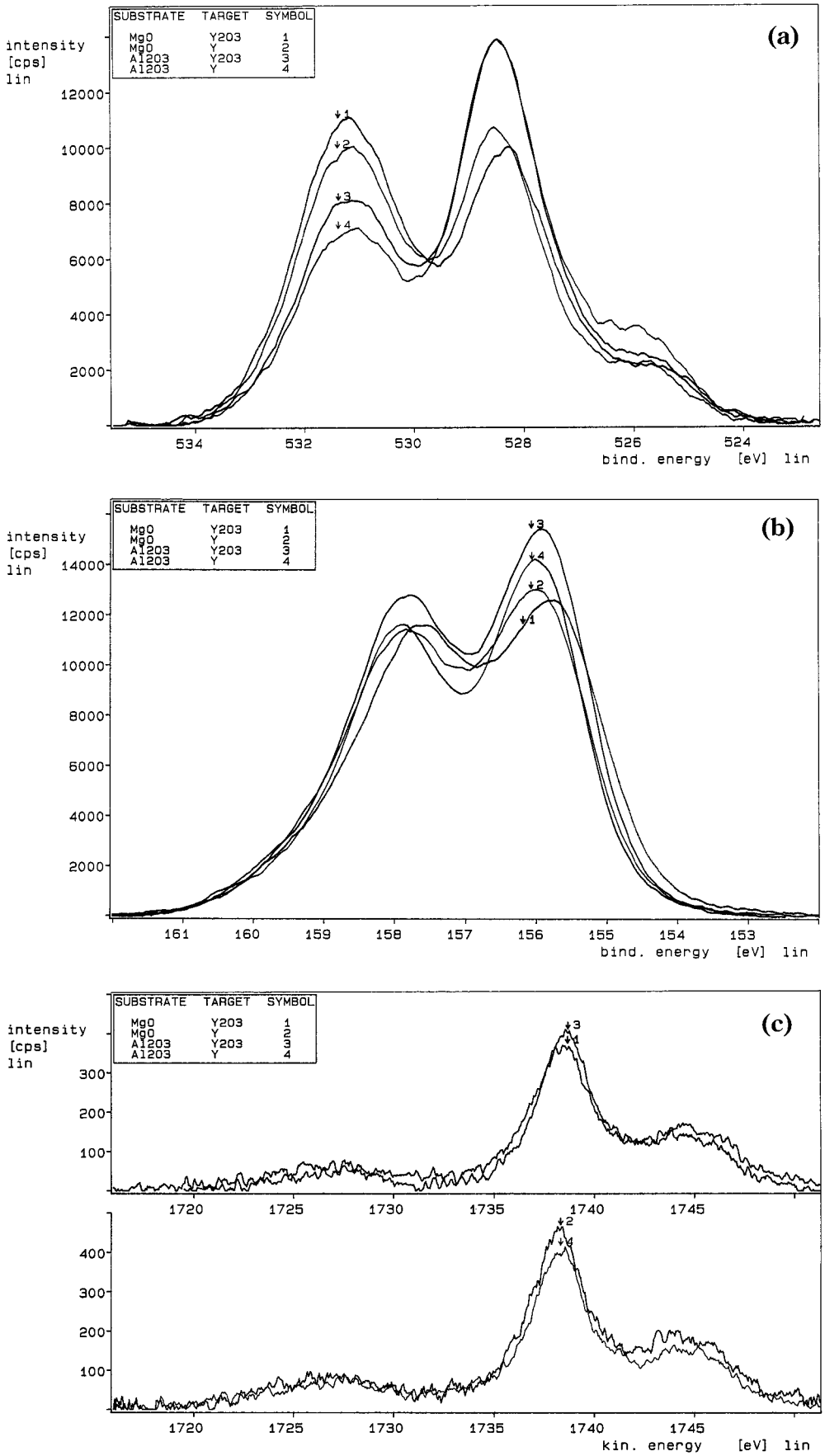

Figure 8. XPS spectra of the (a) O 1s and (b) Y 3d regions and (c) the $L_3M_5M_5$ Y Auger peak (excited by the bremsstrahlung X-ray background) taken from Y_2O_3 films deposited either on MgO(100) or Sapphire(0001) substrate from YO and Y targets.

numeral 2 in Figure 7c). Taking into consideration these two planes with their orientation with respect to each other and to the substrate, the diffraction pattern in Figure 7b can be described. It should also be noted that

other diffraction spots exist in the ED pattern that are a result of the double-diffraction phenomenon.

We should mention that the TEM studies on a Y_2O_3 film grown from the metal target are currently under investigation, but considering the AFM and in-plane ϕ-scan measurements previously described, we expect to observe a similar result. Moreover, the ED patterns taken from both Y- and YO-deposited films on the MgO substrate revealed the same diffraction characteristics, but presented a much lower quality of crystallinity, as observed by the weak and diffuse diffraction spots, which correlates well with the X-ray diffraction studies performed.

X-ray Photoelectron Spectroscopy (XPS). XPS measurements on Y- and YO-deposited films grown on MgO(100) and sapphire(0001) were carried out to study the chemical bonding at the surface of the films. The analyzed samples of the Y_2O_3 films on MgO or sapphire substrate grown from metallic yttrium or yttria target revealed no major chemical differences. The acquired O 1s peak could be fit as two peaks that correspond to the Y−O bond and physisorbed oxygen centered at 528.4 and 531.2 eV, respectively, as shown in Figure 8a.[22] The 525.8 eV peak is due to the sample holder. The attribution of the 531.2 eV peak to physisorbed oxygen was confirmed on a UHV-grown Y_2O_3 film and analyzed in situ without external pollution. The spin−orbit coupling of the Y 3d core level peaks in two states, Y $3d_{3/2}$ and Y $3d_{5/2}$, whose position is around 155.9 eV for the latter with a constant split energy of 2 eV (Figure 8b). The study of intensity points out a slight difference according to the choice of substrate used and displays a better signal for the sapphire substrate. Thus, this signal can reasonably be linked with the better crystalline growth of the films grown on sapphire, as was observed in the X-ray diffraction measurements. Using the O 1s and Y $3d_{5/2}$ Y−O bonded peaks, we attempted to calculate the stoichiometry of the films with a relation based on the formula[31]

$$\frac{X_Y}{X_O} = \frac{y_O}{y_Y}\frac{(1+\beta_O/16)}{(1+\beta_Y/16)}\frac{\sigma_O}{\sigma_Y}\left(\frac{E_Y}{E_O}\right)^{n-1/2}\frac{I_Y}{I_O}$$

where X_I = stoichiometric coefficient, y_I = fraction of photoelectric transition,[31] β_I = asymmetry parameter for Mg K_α X-rays incident on atoms,[32] σ_I = Scofield photoionization cross section,[33] E_I = photoelectron kinetic energy, n = experimental parameter of analyzer, and I_I = peak intensity. With the assumption $y_O = y_Y = 1$, a small deviation in the X_Y/X_O values was observed, yielding 0.68, 0.72, 0.68, and 0.69 and leading, respectively, to the compositions $Y_2O_{2.9}$, $Y_2O_{2.8}$, $Y_2O_{2.9}$, and $Y_2O_{2.9}$ for the Y-deposited films on sapphire and MgO and the YO-deposited films on sapphire and MgO, respectively. Despite a good agreement with results reported by Craciun et al.,[22] we must point out some difficulties. First, in accordance with Wagner,[31] the probability of the shake-up and shake-off phenomenon may induce very low y values for transition metals that are clearly less than unity. On the other hand, a reliable evaluation of the Y 3s and Y $3p_{3/2}$ peaks gives different results that yield values that are lower and higher, respectively, than the stoichiometric value. A second attempt was made to characterize the oxidation state of the samples with the modified Auger parameter based on the Y $3d_{5/2}$ and $L_3M_5M_5$ peaks using $\alpha' = E_{B(}$Y 3d) + E_K(LMM). The mean energies values for the films deposited on MgO and sapphire substrate were 1894.1 and 1894.3 eV, respectively. These values lie between those reported by Durand et al.[30] for oxygen-rich and oxygen-deficient Y_2O_3 thin-film samples, which showed values of 1893.2 and 1894.8 eV, respectively, thus suggesting that our Y_2O_3 films are slightly oxygen-deficient with either an Y_2O_{3-x} or an ($xY + Y_2O_3$) film representation. However, it is worth mentioning that films deposited from the metal target have the same stoichiometry as films deposited from the yttria target, and no obvious differences were observed between films deposited from either target.

IV. Conclusions

We have shown for the very first time, through morphological and structural investigations, that the use of yttrium metal as an ablation target for the deposition of Y_2O_3 films via PLD provides a convenient and effective alternative to the traditionally employed Y_2O_3 ablation target. The Y_2O_3 films deposited from the metal target exhibited a deposition rate approximately 23% higher than that of the YO-deposited films while maintaining a higher crystallinity and smoother film surface, as confirmed by AFM and SEM measurements. The TEM investigations confirmed that, although the films contain two in-plane orientations with respect to the substrate, higher-quality films were obtained from Y-deposited films on the sapphire substrate. From the XPS investigations, we concluded that no significant difference was existed between the films deposited from the metallic and oxide targets, thus inferring that the same degree of oxidation was obtained in films deposited from either target. The reason for the slightly higher crystallinity of the Y_2O_3 films deposited from the metal target versus those deposited from the oxide target is not completely understood. Therefore, spectroscopic investigations on the laser-ablated plasma are currently underway to help gain insight into the growth process of Y_2O_3 films in hopes of optimizing the growth and obtaining single in-plane epitaxy.

Acknowledgment. The authors gratefully acknowledge the financial support of the CNRS (France) and the STCS for funding this work. We also extend gratitude to Professor M. Hervieu for help in resolving the TEM data, Dr. D. Grebille for fruitful crystallography discussions, and M. Morin for preparation of the cross-section samples of films for the electronic microscopy investigations.

CM001094E

(30) Duraud, J. P.; Jolet, F.; Thromat, N.; Gautier, M.; Maire, P.; le Gressus, C.; Dartyge, E. *J. Am. Ceram. Soc.* **1990**, *73*, 2467.
(31) Wagner, C. D. *Anal. Chem.* **1997**, *49* (9), p1282.
(32) Reilman, R. F.; Bezane, A. M.; Manson, S. T. *J. Electron Spectrosc. Relat. Phenom.* **1976**, *8*, 389.
(33) Scofield, J. H. *J. Electron Spectrosc. Relat. Phenom.* **1976**, *8*, 129.